Lattice Imaging of Electro-Optically Active Poly(nonylbithiazole) (PNBT)

L. González Ronda and D. C. Martin*

Macromolecular Science and Engineering Center and Department of Materials Science and Engineering, 2022 H. H. Dow Building, The University of Michigan, Ann Arbor, Michigan 48109-2136

Received October 1, 1996

Revised Manuscript Received January 21, 1997

Introduction. Processable conjugated polymers have been a topic of intense research for the past several years due to their potential use as the active layers of light-emitting diodes (LEDs),[1] chemical sensors,[2] and thin-film transistors.[3] Considerable efforts have been made to understand the relationship between the structure and electro-optical[4−7] and mechanical properties[8,9] of polymers such as the poly(3-alkylthiophene)s (P3ATs).[5,10−13] Moulton and Smith studied the mechanical and electrical properties of P3ATs as a function of alkyl chain length and found that their differences in conductivity and tensile modulus could be explained by changes in the density of covalent bonds and by a decrease in $\pi-\pi$ overlaps due to a stereo-irregular polymer structure.[8,9] McCullough et al. demonstrated the importance of stereo-regularity in increasing backbone planarity and conductivity by comparing P3ATs synthesized by conventional and regiospecific methods.[6] A decrease in conductivity of both stereo-regular and stereo-irregular P3ATs has been observed in morphologically rough thick films.[4,6] Yassar et al. found that increasing the thickness of electrochemically polymerized films augmented chain disorder and decreased conjugation length.[4] The loss of chain order has also been shown to cause dramatic thermo- and solvatochromic effects in P3ATs, whose optical absorption maxima (λ_{max}) decrease sharply either with increasing temperature or through solvent interactions,[5,7,10,14] In poly(nonylbithiazole) (PNBT), an increase in λ_{max} has been observed and correlated with ordering during crystallization.[15]

The work presented here demonstrates the suitability of high-resolution electron microscopy (HREM) to study the morphology of poly(bithiazole)s (PBTs). PBTs are of interest because unlike most conjugated polymers, they can exhibit n-type electrical conductivity. N-doping is made possible by the π-deficient nature of the imine nitrogens in the bithiazole units and may lead to the use of PBTs as electron injection layers in LEDs.[16,17] Our goal is to determine the influence of microstructure on the macroscopically observed properties of these polymers in order to optimize device performance.

HREM has been successfully used to study similar systems. Lovinger presented HREM images of intermolecular packing in hexyl-substituted α-hexathienylene (α-6T).[18] Voigt-Martin et al. used HREM to study the molecular organization of sanidic polyamides, a family of board-shaped polymers composed of stiff aromatic backbones and solubilizing alkyl side groups.[19] Here, we report the successful HREM imaging of the 2.4 nm (100) lattice fringes of PNBT and subsequent observations regarding the size, shape, orientation, and distortion of its crystals.

Experimental Procedure. Stereoregular poly(nonylbithiazole)

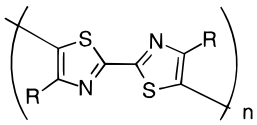

R = nonyl

was synthesized by Curtis et al. from the brominated halomethyl ketone and dithiooxamide by dehalogenative coupling with nickel in refluxing toluene.[15] Molecular weights of $M_n = 22\,000$ and $M_w = 44\,000$ were measured using gel permeation chromatography. A 0.01 weight percent solution of PNBT in chloroform was filtered through a 0.45 mm Millipore membrane and atomized over carbon-coated mica sheets. The coated mica sheets were then heated to 220 °C at a rate of 10 °C/min, held at 220 °C for 4 h, and cooled to room temperature at 0.5 °C/min. The PNBT-coated carbon film was removed from the mica by submerging the sheets into deionized water. TEM specimens were prepared by lifting the floating films with 400 mesh copper grids. The samples were allowed to air dry overnight.

A JEOL 4000EX operated at 350 kV was used for low-dose HREM analysis of the annealed PNBT samples. Conditions for searching, focusing, and photographing the samples were preset using a minimum dose system. The critical dose for these samples was calculated to be 0.013 C/cm^2 based on the empirical relationship by Kumar and Adams that correlates a polymer's beam damage resistance to its melting or degradation temperature.[20] Successful imaging conditions required a magnification of 30000×, a beam current of 13.0 pA/cm^2, and an exposure time of 1.0 s. The optimum defocus for imaging the 2.4 nm (100) lattice fringes was calculated from the relationship

$$\Delta f = d^2/2\lambda$$

where d is the lattice spacing of the material and λ is the electron wavelength.[21] The lattice spacings were calibrated using a He−Ne optical bench and lattice images of graphitized carbon black ($d = 0.34$ nm).

The sizes, shapes, and internal perfection of the PNBT crystallite domains were determined by visual inspection, as has been described elsewhere.[22] We also quantified lattice fringe orientation with the aid of the public domain software NIH Image (available at http://rsb.info.nih.gov/nih-image/). Crystallite dimensions were determined by measuring along the main chain axis (parallel to the (100) fringes) and in the lateral packing direction (perpendicular to the (100) fringes). Internal distortions of the crystals were estimated from the local radius of curvature of continuous fringes within individual domains. The orientation was measured relative to the nearest surface, evident as a slight variation in contrast relative to the carbon substrate.

Results and Discussion. The annealed PNBT droplets were discontinuous, rough, and contained numerous holes. A HREM image of the 2.4 nm (100) intermolecular spacing of PNBT is shown in Figure 1. This spacing corresponds to the intermolecular, side-to-side distance between the backbones of polymer chains, which are separated by two sets of alkyl chains (Figure 2).[15] Multislice calculations predict that the darker lines in the HREM image correspond to the polymer backbone, which has a higher projected electron potential.[23] The orientation of these (100) fringes was

S0024-9297(96)01456-8 CCC: $14.00

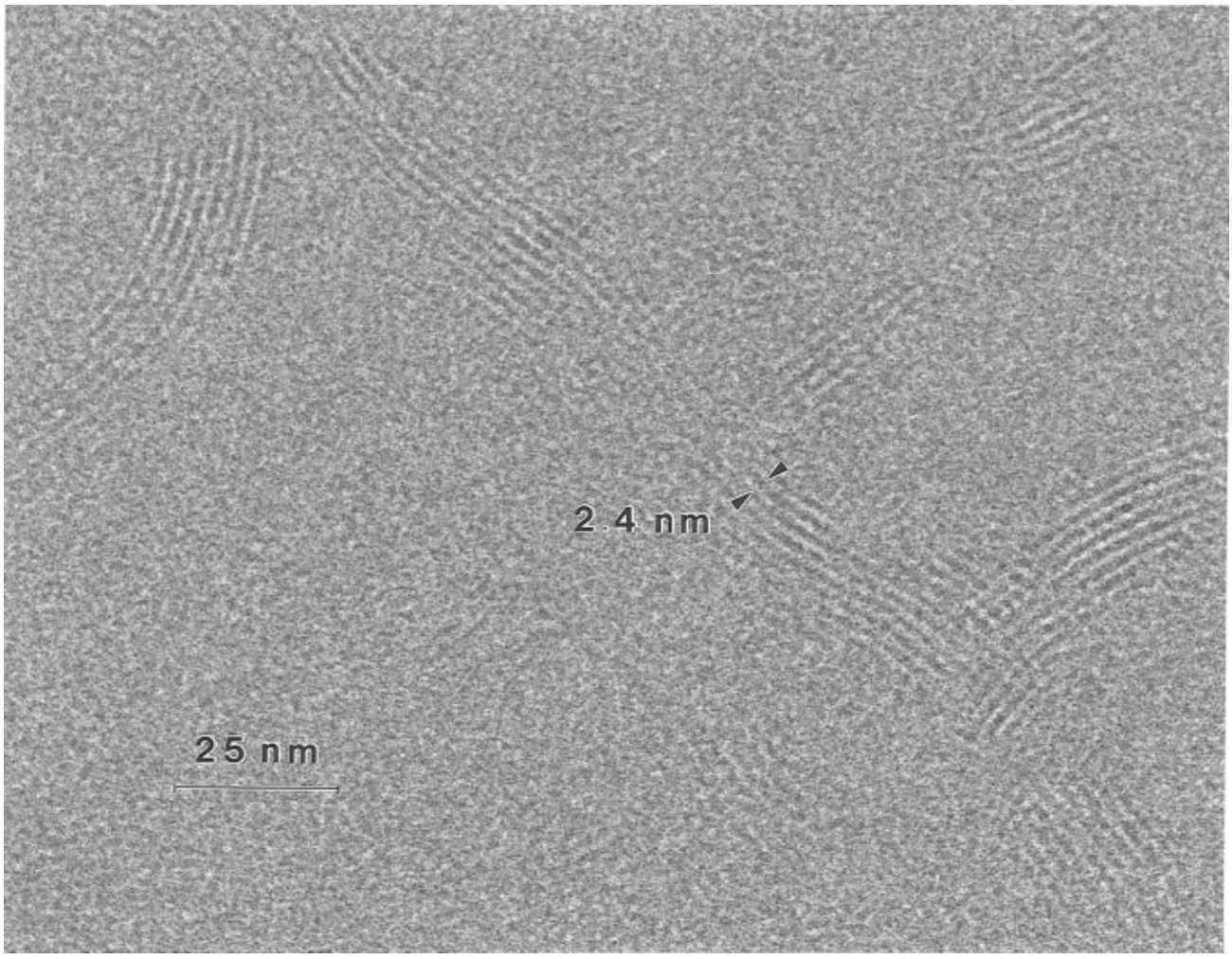

Figure 1. High-resolution electron microscopy image of poly(nonylbithiazole). The lattice fringes correspond to the side-to-side distance between chains, 2.4 nm.

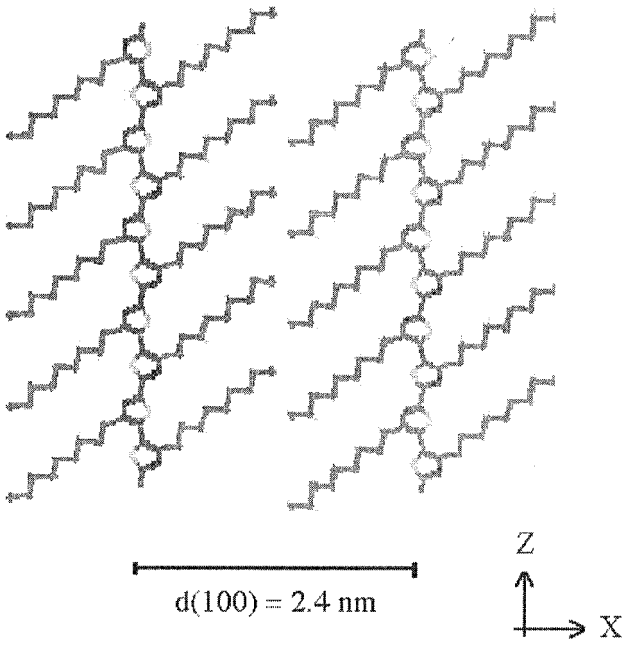

Figure 2. Schematic of the crystalline arrangement of poly(nonylbithiazole) chains.

observed to be sensitive to the presence of free surfaces: crystallites were more numerous near sample edges and their (100) planes preferentially aligned parallel to the nearest surface, as shown in Figure 3.

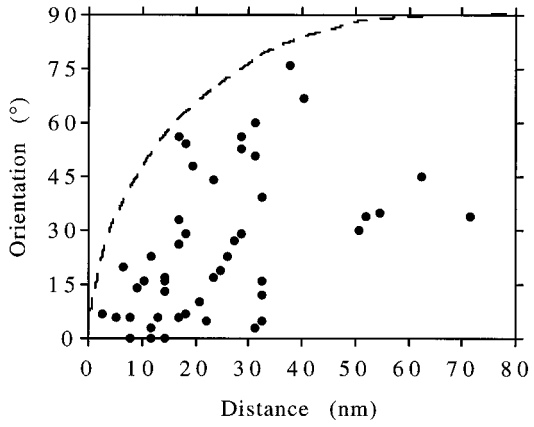

Figure 3. Orientation of the (100) lattice fringes in poly(nonylbithiazole) as a function of distance from the nearest surface. Crystallites near the surface align preferentially parallel to the edge and become increasingly misoriented with distance, as outlined by the dashed curve.

The average projected crystallite size was measured to be 13 ± 6 nm wide (perpendicular to the chain axis) and 14 ± 9 nm tall (along the chain axis) (Figure 4).

Evidence for considerable local bending of the PNBT lattice about the [010] direction was obtained, with some local radii of curvature as small as 12 nm (Figure 1). Our data indicated that the bent PNBT crystallites tended to be somewhat longer than they are wide, resulting in a typical aspect ratio of 1.3. Lattice bending

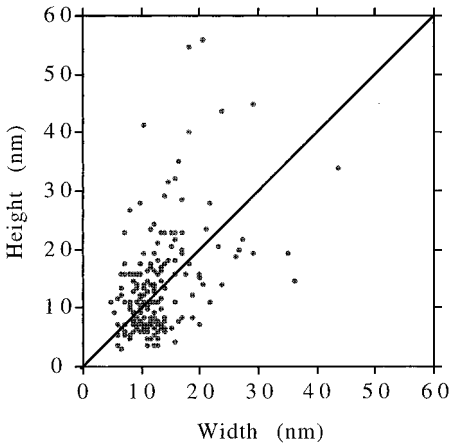

Figure 4. Distribution of the projected crystallite dimensions of poly(nonylbithiazole). Heights and widths were measured parallel and perpendicular to the (100) fringes, respectively.

was observed in approximately 10% of the crystallites examined, both near surfaces and in the bulk. Such severe lattice deformation has important implications for the properties of conjugated polymers, since bending of the (100) planes may necessitate the systematic presence of [001] dislocations to accommodate the distortion.[24,25] These dislocations would in turn disturb backbone planarity and inhibit charge transport.[26,27] Calculations by Brédas et al. have predicted a decrease in bandwidth and increases in the ionization potential and bandgap of polythiophene as a function of the torsion angle between adjacent thiophene rings.[27] Further analysis of the energetics of bending deformation in poly(bithiazole) crystals will help quantify the effects of these distortions on their electrical properties and the associated effects on device performance.

Acknowledgment. The authors are grateful to Dr. M. David Curtis, John I. Nanos, and Jo A. Johnson for providing the PNBT used in this study. This work was supported by the University of Michigan Display Technology and Manufacturing Center and the National Science Foundation (NYI Award DMR-9257569). L.G.R. would also like to thank the University of Michigan Rackham School of Graduate Studies for fellowship support.

References and Notes

(1) Braun, D.; Guftasson, G.; McBranch, D.; Heeger, A. J. *J. Appl. Phys.* 1992, *72*, 564.
(2) Bidan, G. *Sens. Actuators B* **1992**, *6*, 45.
(3) Garnier, F.; Hajlaoui, R.; Yassar, A.; Srivastava, P. *Science* **1994**, *265*, 1684.
(4) Yassar, A.; Roncali, J.; Garnier, F. *Macromolecules* **1989**, *22*, 804.
(5) Tashiro, K.; Ono, K.; Minagawa, Y.; Kobayashi, M.; Kawai, T.; Yoshino, K. *J. Polym. Sci., Part B: Polym. Phys.* **1991**, *29*, 1223.
(6) McCullough, R. D.; Lowe, R. D. *J. Chem. Soc., Chem. Commun.* **1992**, 70.
(7) Roux, C.; Leclerc, M. *Macromolecules* **1992**, *25*, 2141.
(8) Moulton, J.; Smith, P. *Synth. Met.* **1991**, *40*, 13.
(9) Moulton, J.; Smith, P. *Polymer* **1992**, *33*, 2340.
(10) Winokur, M. J.; Spiegel, D.; Kim, Y.; Hotta, S.; Heeger, A. J. *Synth. Met.* **1989**, *28*, C419.
(11) Gustafsson, G.; Inganäs, O.; Österholm, H.; Laakso, J. *Polymer* **1991**, *32*, 1574.
(12) Prosa, T. J.; Winokur, M. J.; Moulton, J.; Smith, P.; Heeger, A. J. *Macromolecules* **1992**, *25*, 4364.
(13) Mårdalen, J.; Samuelsen, E. J.; Gautun, O. R.; Carlsen, P. H. *Synth. Met.* **1992**, *48*, 363.
(14) Inganäs, O.; Salaneck, H. R.; Österholm, J. E.; Laakso, J. *Synth. Met.* **1988**, *22*, 395.
(15) Nanos, J. I.; Kampf, J. W.; Curtis, M. D.; Gonzalez, L.; Martin, D. C. *Chem. Mater.* **1995**, *7*, 2232.
(16) Newkome, G. R.; Paudler, W. W. *Contemporary Heterocyclic Chemistry*; Wiley: New York, 1982.
(17) Yamamoto, T.; Suganuma, H.; Maruyama, T.; Kubota, K. *J. Chem. Soc., Chem. Commun.* **1995**, 1613.
(18) Lovinger, A. *Bull. Am. Phys. Soc.* **1996**, *41* (1), 46.
(19) Voigt-Martin, I. G.; Simon, P.; Bauer, S.; Ringsdorf, H. *Macromolecules* **1995**, *28*, 236.
(20) Kumar, S.; Adams, W. W. *Polymer* **1990**, *31*, 15.
(21) Martin, D. C.; Thomas, E. L. *Polymer* **1995**, *36*, 1743.
(22) Martin, D. C.; Berger, L. L.; Gardner, K. H. *Macromolecules* **1991**, *24*, 3921.
(23) Molecular Simulations, Inc. Cerius^2 Molecular Modelling Software, Version 2.0 (1996).
(24) Nye, J. F. *Acta Metall.* **1953**, *1*, 153.
(25) Wilson, P. M. Ph.D. Thesis, University of Michigan, 1994.
(26) Liao, J.; Martin, D. C. *Macromolecules* **1996**, *29*, 568.
(27) Brédas, J. L.; Street, G. B.; Thémans, B.; André, J. M. *J. Chem. Phys.* **1985**, *83*, 1323.

MA961456X